

Electron Affinities from Electron-Transfer Equilibria: $A^- + B = A + B^-$

Eric P. Grimsrud,[†] Gary Caldwell, Swapan Chowdhury, and Paul Kebarle*

Contribution from the Chemistry Department, University of Alberta, Edmonton, Alberta, Canada T6G 2G2. Received December 26, 1984

Abstract: Determination of the equilibrium constants K_1 for gas-phase electron-transfer equilibria [$A^- + B = A + B^-$ (1)] with a pulsed electron beam high ion source pressure mass spectrometer led to the electron affinities of 34 compounds with EA's between 0.5 and 3 eV. The compounds are mostly substituted nitrobenzenes, substituted quinones, and conjugated molecules containing oxygen atoms. The EA of smaller molecules like SO_2 , NO_2 , CS_2 , and CH_3NO_2 also were determined. The method is very well suited for rapid, accurate, routine determinations of electron affinities. A comparison with EA's determined with other gas-phase methods and EA's evaluated from polarographic half-wave reduction potentials and charge-transfer spectra in solution is made. The rate constants for a number of exothermic electron-transfer reactions were determined. Most of these proceed at near collision rates. Electron-transfer reactions involving perfluorinated compounds like perfluoromethylcyclohexane, perfluorocyclohexane, and sulfurhexafluoride do not follow this behavior. While the perfluoro compounds have high thermal electron capture cross sections, they do not accept electrons from A^- of compounds A with lower electron affinity. The perfluoro anions do transfer electrons to compounds A with higher electron affinity, and the rate constants increase with $EA(A) - EA(\text{perfluoro compound})$.

The electron affinities of molecules are of interest not only in areas where gas-phase ions are encountered, e.g., ionosphere, gaseous electronics, gas-phase radiation chemistry, electron capture detector for gas chromatography, negative ion analytical mass spectrometry, and gas-phase ion chemistry, but also in the much wider field of condensed-phase chemistry. Charge-transfer complexes and their role in organic, catalytic, and biological processes represent an example of a vast condensed phase area for which knowledge of electron affinities is of prime importance. The review articles by Szwarc¹ and Briegleb² provide very informative overviews of the broad range of EA applications to condensed-phase chemistry.

In spite of the fundamental significance of electron affinities, until relatively recently electron affinity data were very scarce. For example, the compilation by Vedenev³ (1966) contained the electron affinities of not many more than 10 molecules and these had rather large error limits. Fortunately, the situation has been improving rapidly. Important contributions to the pool of EA data were the determinations of Chen and Wentworth⁴ with an electron-capture detector and the correlations by Batley and Lyons,⁵ Briegleb,² and Chen and Wentworth⁶ of gas-phase electron affinities with solution electron affinities based on spectral properties of charge-transfer complexes and polarographic half-wave reduction potentials. Most important was the rapid development of physical methods for EA determinations in the gas phase reviewed by Chen and Wentworth⁶ and particularly the photodetachment methods reviewed recently by Brauman et al.⁷ and Lineberger et al.⁸ Brauman's article contains an up to date tabulation of electron affinities determined by physical methods which contains some 50 molecules. In spite of these recent advances, when one considers that the electron affinities of many hundreds of molecules are needed, it becomes clear that methods for the rapid, reliable determination of electron affinities are still very desirable. Ion-molecule equilibria measurements in the gas phase⁹ have become a major source of gas-phase thermochemical data like proton affinities, ion-ligand binding energies, gas-phase acidities, etc. The ion-molecule equilibrium method can be applied also toward the determination of electron affinities. McIver and Fukuda¹⁰⁻¹² were the first to show that the electron-transfer equilibria 1 can be measured in the gas phase. Once such



measurements are possible, the evaluation of thermochemical data follows established procedures.⁹ Measurement of the relative

concentrations of A^- and B^- at equilibrium, together with the known concentrations of the neutral A and B, leads to an evaluation of the equilibrium constant K_1 , see eq 2 and ΔG°_1 via eq 3. Since ΔS°_1 is expected to be very small,^{11,38} (4) leads to (5)

$$K_1 = \frac{[B^-][A]}{[A^-][B]} \quad (2)$$

$$-RT \ln K_1 = \Delta G^\circ_1 \quad (3)$$

$$\Delta G^\circ_1 = \Delta H^\circ_1 - T\Delta S^\circ \quad (4)$$

$$\Delta G^\circ_1 \approx \Delta H^\circ_1 \approx \Delta E^\circ_1 = EA(A) - EA(B) \quad (5)$$

which means that determination of equilibria 1 provides relative thermal electron affinities. Measurements of a number of equilibria 1 involving different compounds with progressively changing EA's permit the construction of a ladder of interconnecting ΔH°_1 results (see, for example, Figure 1 in Results and Discussion), and the electron affinities of all the compounds which are part of the continuous ladder can be determined, provided the EA of one compound, external standard or anchor, is known. Fukuda and McIver¹⁰ using a pulsed, ion trapped ion cyclotron resonance mass spectrometer established such a ladder involving some 15 compounds, the majority being nitrobenzenes and quinones. Unfortunately, they did not anchor their ladder to a compound whose EA was well established in the literature, but they chose a procedure¹¹ which led to an erroneous anchoring of the scale. More recently Caldwell and Kebarle¹³ measured equilibria 1 with a pulsed electron beam high pressure mass spectrometer. They were able to reproduce closely the ΔH°_1 measured by Fukuda and McIver.¹⁰⁻¹² By comparing the resulting ladder of relative electron affinities to absolute EA's from the literature, they were able to anchor the ladder and observe good

(1) Szwarc, M. *Prog. Phys. Org. Chem.* **1968**, *6*, 323.

(2) Briegleb, G. *Angew. Chem. Int. Ed. Engl.* **1964**, *3*, 617.

(3) Vedenev, V. I., et al. "Bond Energies, Ionization Potentials and Electron Affinities"; Edward Arnold Publishers: London, 1966.

(4) Chen, E. C. M.; Wentworth, W. E. *J. Phys. Chem.* **1983**, *87*, 45.

(5) Batley, M.; Lyons, L. E. *Nature (London)* **1962**, *196*, 573.

(6) Chen, E. C. M.; Wentworth, W. E. *J. Chem. Phys.* **1975**, *63*, 3183.

(7) Drzagic, P. S.; Marks, J.; Brauman, J. I. "Electron Photodetachment from Gas Phase Molecular Ions" in "Gas Phase Ion Chemistry"; Bowers, M. T., Ed.; Academic Press: New York, 1984; Vol. 3.

(8) Mead, R. D.; Stevens, A.; Lineberger, W. C. "Photodetachment in Negative Ion Beams"; Academic Press: New York, 1984.

(9) Hogg, W. M.; Kebarle, P. *J. Chem. Phys.* **1965**, *40*, 449. Kebarle, P. *Annu. Rev. Phys. Chem.* **1977**, *28*, 445. Henderson, W. G.; Taagepera, D.; Holtz, D.; McIver, R. T.; Beauchamp, J. L.; Taft, R. W. *J. Am. Chem. Soc.* **1972**, *94*, 4728.

(10) McIver, R. T.; Fukuda, E. K. "Lecture Notes in Chemistry"; Hartman, H.; Wanzek, K. P., Eds.; Springer: Berlin, 1982; p 164.

(11) Fukuda, E. K.; McIver, R. T. *J. Chem. Phys.* **1982**, *77*, 4942.

(12) Fukuda, E. K.; McIver, R. T. *J. Phys. Chem.* **1983**, *87*, 2993.

(13) Caldwell, G.; Kebarle, P. *J. Chem. Phys.* **1984**, *80*, 1.

[†] Visiting scientist on sabbatical leave. Permanent address: Chemistry Department, Montana State University, Bozeman, Montana 59717.

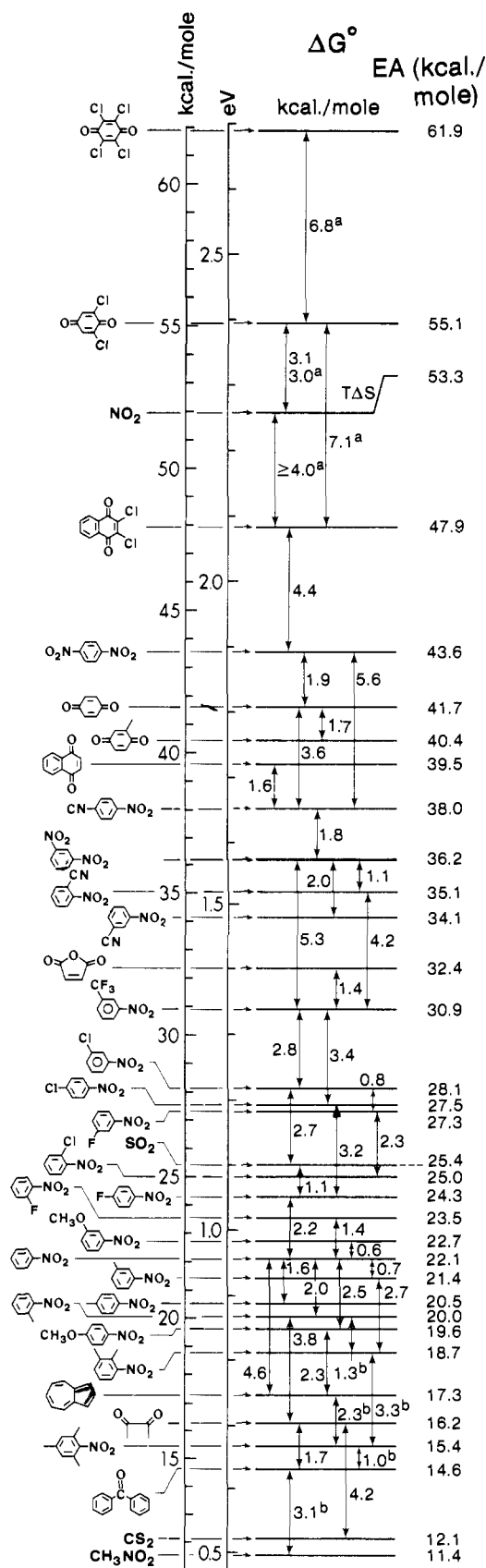


Figure 1. Electron affinities³⁸ from equilibria 1 ($A^- + B = A + B^-$) measurements. ΔG°_1 are given between double arrows connecting A and B for each equilibrium measured. All equilibria unless otherwise indicated were measured at 150 °C: (a) 215 °C, (b) 80 °C. Absolute electron affinities were obtained by anchoring to literature value²¹ EA-(SO₂) = 1.1 eV.

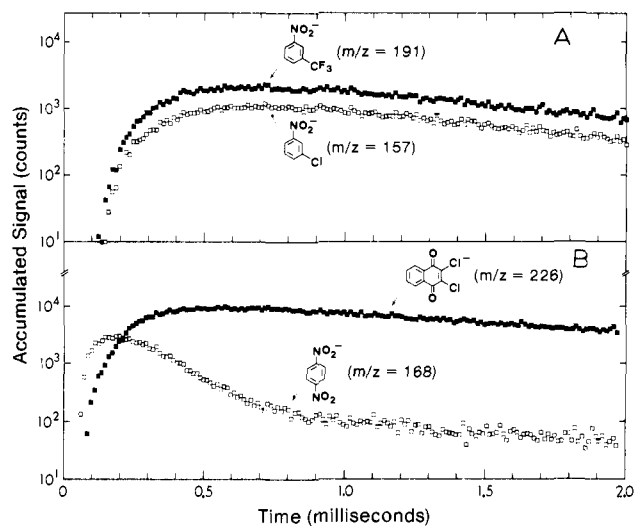


Figure 2. Ion intensities as a function of time after a 10- μ s electron pulse. Ion source temperature 150 °C. Figure A, ions have reached equilibrium 1 already at onset of ion signal. Constant $[A^-]/[B^-]$ ratio corresponds to constant vertical distance between A⁻ and B⁻; 3.5 torr of CH₄, 0.53 mtorr of *m*-(trifluoromethyl)nitrobenzene, 7.6 mtorr of *m*-chloronitrobenzene. Figure B, equilibrium 1 is reached after about 0.9 ms; 2.8 torr of CH₄, 0.54 mtorr of *p*-dinitrobenzene, 0.49 mtorr of 2,3-dichloronaphthoquinone.

agreement with several reliable EA's from the literature.

The present work is an extension of the earlier measurements.¹³ The new, extended ladder provides EA's for some 36 compounds covering an energy span of 50 kcal/mol (~ 2 eV). In the subsequent text we provide information on the measurement conditions and the kinetics of a number of electron-transfer reactions 1 and also discuss the significance of the measured electron affinities.

Experimental Section

The measurements of equilibria 1, $A^- + B = A + B^-$, were executed with a pulsed electron beam, high ion source pressure mass spectrometer which has been described previously.¹⁴ The same instrument was used as in the earlier work¹³ on equilibria 1. All the compounds were the highest purity available from commercial suppliers. They were used without further purification. Impurities which affect the measurements are detected by the observation of the negative ions that are formed due to their presence. The only serious difficulty with impurities occurs when measurements with a compound B are performed which contains as impurity an isomer B' of higher electron affinity. This may lead to an apparent EA value that is higher than the true value. For this to happen the impurity has to be more than 10%. The presence of lesser amounts of isomeric impurity are detectable. One observes a very slow approach to the (false) $([B^-] + [B'^-])/[A^-]$ equilibrium since the concentration of B' isomer is low and this leads to a slow approach to the apparent equilibrium.

Results and Discussion

(a) Kinetics of the Electron-Transfer Reactions—Well Behaved and Very Slow Electron Transfer. The thermochemical data and the electron affinities resulting from measurement of the electron transfer equilibria 1 are given in Figure 1. The significance of these data will be discussed in the next section. Shown in Figure



2 is the observed time dependence of ions in two typical experiments. Figure 2A shows a situation where B (3-(trifluoromethyl)nitrobenzene) has an electron affinity which is 2.8 kcal/mol higher than A (2-chloronitrobenzene). The natural concentration ratio $[A^-]/[B^-] = 14.3$ was chosen to offset the advantage of the higher EA(B) which promotes high $[B^-]$ at equilibrium. The ions appear after about a 0.1-ms delay. The ratio $[B^-]/[A^-]$ which, in the log plot used, is given by the vertical distance between the

(14) Cunningham, A. J.; Payzant, J.; Kebarle, P. *J. Am. Chem. Soc.* **1972**, *94*, 7627.

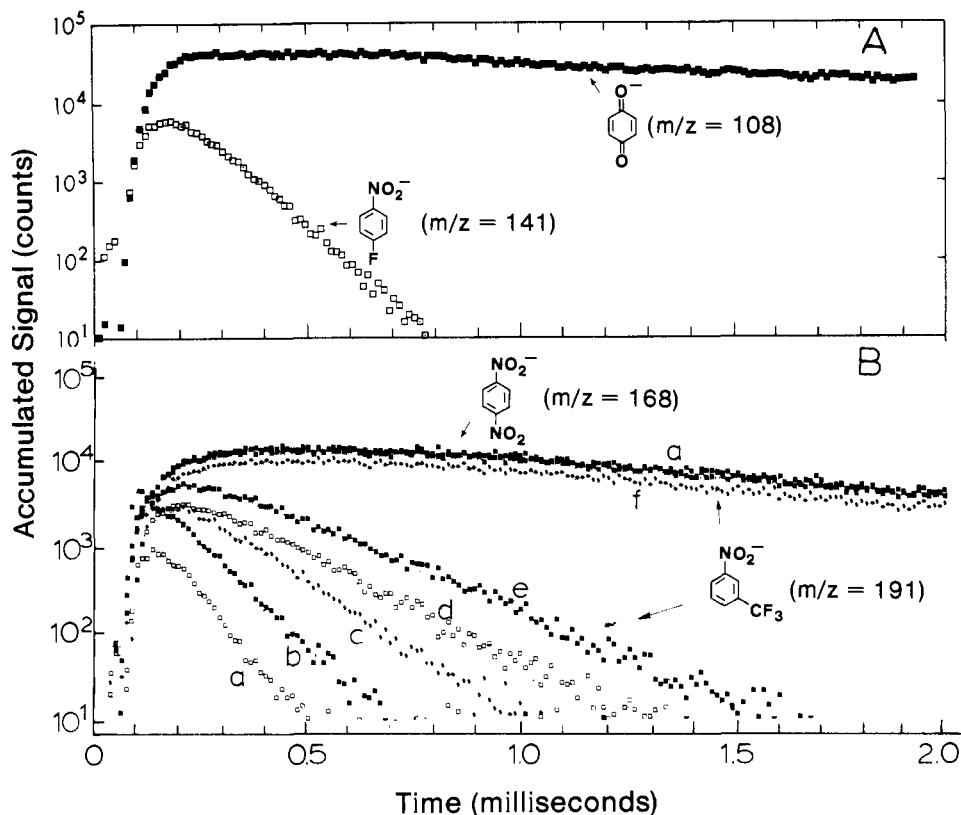


Figure 3. (A) Concentration changes due to electron transfer from *p*-fluoronitrobenzene anion to higher electron affinity benzoquinone. The slope of the linear portion of the nitrobenzene anion decay can be used for determination of rate constant for electron transfer; 2 torr of fluoronitrobenzene, 0.3 torr of benzoquinone, 4 torr of CH_4 . (B) Electron transfer from *m*-(trifluoromethyl)nitrobenzene anion to higher electron affinity *p*-dinitrobenzene. The slopes of the linear portion of decaying (trifluoromethyl)nitrobenzene anion = $\nu_1(\text{obsd})$ are used for determination of rate constant k_1 (see Figure 4); *m*-(trifluoromethyl)nitrobenzene, 15 torr; CH_4 , 4 torr; *p*-dinitrobenzene at different pressures; a 0.5, b 0.33, c 0.25, d 0.167, e 0.116, f = mtorr; temp = 150 °C. Accumulated signal for *p*-dinitrobenzene anion is almost identical for cases a-f, so only case a is shown.

two ion intensity curves is observed to be essentially constant from the very onset of the ions. This means that the equilibrium 1 was achieved already within the short 0.1 ms time before the ions started emerging from the ion source. Another interpretation of the results in Figure 2A is also possible, namely that the reaction 1 is so slow that no reactive change whatever is occurring within the ~ 2 ms time available for the observation. Since ion diffusion to the wall of the ion source is the main ion loss mechanism,¹⁵ a constant ratio in the "very slow"-no equilibrium case would be observed only when the diffusion coefficients of A^- and B^- are very similar.

The intensities displayed in Figure 2B show clearly concentration changes due to reaction 1. The 1,4-dinitrobenzene has a 4.4 kcal/mol lower EA than the naphthoquinone, and since the neutral concentrations were chosen to be nearly equal, the nitrobenzene anion is seen to decrease for some 0.7 ms with the two log curves becoming equidistant after that time. The results in this figure show the kinetics of the approach to the equilibrium and the constant concentration ratio after the equilibrium was achieved. The slope of the initial linear section of the dinitrobenzene curve can be used to obtain an approximate rate constant for the electron-transfer reaction to naphthoquinone. To obtain more accurate rate constants, longer linear sections are desirable and these can be obtained when compound B is of much higher electron affinity than A such that A^- disappears essentially completely. An example of such a run is shown in Figure 3A where the log $[\text{A}^-]$ plot has a long linear section. The slope of this section when converted to the natural logarithm by multiplying with 2.303 equals $\nu_1(\text{obsd})$, the observed pseudo-first-order rate constant for A^- disappearance. This is given by eq 6 where ν_{d,A^-} is the first-order rate constant for loss of A^- by diffusion to the walls. Choosing different $[\text{B}]$ in a series of experiments at constant T

$$\nu_1(\text{obsd}) = k_1[\text{B}] + \nu_{d,\text{A}^-} \quad (6)$$

one obtains a series of slopes $\nu_1(\text{obsd})$ as shown in Figure 3B. The

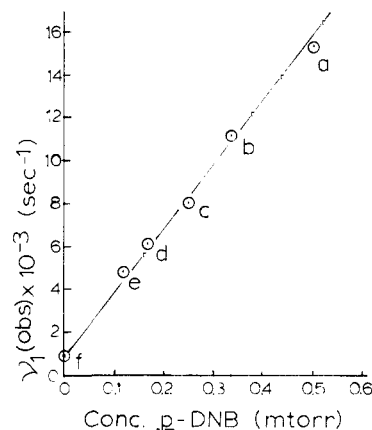


Figure 4. Plot of $\nu_1(\text{obsd})$, from Figure 3B, vs. concentration of *p*-dinitrobenzene. The slope of the present plot gives the rate constant k_1 while the intercept gives the rate constant ν_{d,A^-} for diffusional loss to the wall (see eq 6 in text).

$\nu_1(\text{obsd})$ obtained from this series can then be plotted vs. the known $[\text{B}]$ (see Figure 4). The straight line obtained has a slope which equals k_1 and an intercept equalling ν_{d,A^-} . The above procedure leads to the most accurate k_1 determinations obtainable with our apparatus. When large $[\text{B}]$ are used ν_{d,A^-} is very much smaller than $k_1[\text{B}]$ (see Figure 4). Under such conditions, quite accurate ($\pm 20\%$) rate constants k_1 can be obtained by determining $\nu_1(\text{obsd})$ at a given large $[\text{B}]$ concentration and then assuming $\nu_{d,\text{A}^-} \approx \nu_{d,\text{B}^-}$ and evaluating k_1 from (6). The diffusion rate constant ν_{d,B^-} is available from the constant slope of $\ln [\text{B}^-]$ at long reaction times (see Figure 3). The very similar slopes of A^- for $[\text{B}] = 0$ and B^- at long reaction times, Figure 3, illustrate that the two diffusion rate constants are close when the masses of A^- and B^- are close. The experimental k_1 given in Table I were obtained mostly with

Table I. Rate Constants for Exothermic Electron-Transfer Reactions (Eq 1): $A^- + B = A + B^-$

	A ^a	B ^a	k _(exptl) ^b	k _{1(ADO)} ^c		A ^a	B ^a	k _{1(exptl)}
1	NB	<i>p</i> -NO ₂ NB	1.3	1.1	16	<i>p</i> -NO ₂ NB	2,3-Cl ₂ (naph Q)	0.4
2	NB	<i>m</i> -NO ₂ NB	2.1	1.8	17	2,3-Cl ₂ (naph Q)	2,6-Cl ₂ Q	1.5
3	<i>m</i> -CF ₃ NB	<i>p</i> -NO ₂ NB	1.3	1.0	18	2,6-Cl ₂ Q	Cl ₄ Q	0.5
4	<i>p</i> -FNB	<i>m</i> -NO ₂ NB	1.9	1.8	19	C ₇ F ₁₄	2,6-Cl ₂ Q	0.8
5	NB	<i>m</i> -CF ₃ NB	1.8	1.8	20	C ₇ F ₁₄	NO ₂	0.08
6	<i>p</i> -MeNB	<i>m</i> -CF ₃ NB	1.9	1.7	21	C ₇ F ₁₄	<i>p</i> -NO ₂ NB	0.4
7	NB	NO ₂	0.4	0.6	22	C ₇ F ₁₄	<i>m</i> -NO ₂ NB	0.1
8	<i>p</i> -CH ₃ NB	NO ₂	0.5	0.6	23	C ₇ F ₁₄	<i>m</i> -CF ₃ NB	0 ^d
9	<i>p</i> -ClNB	NO ₂	0.5	0.6	24	C ₇ F ₁₄	<i>m</i> -ClNB	0 ^d
10	<i>m</i> -NO ₂ NB	NO ₂	0.5	0.6	25	C ₇ F ₁₄	<i>p</i> -FNB	0 ^d
11	<i>p</i> -NO ₂ NB	NO ₂	0.4	0.6	26	C ₇ F ₁₄	NB	0 ^d
12	Q	NO ₂	0.3	0.5	27	<i>m</i> -CF ₃ NB	C ₇ F ₁₄	0 ^d
13	azulene	<i>m</i> -CF ₃ NB	1.0		28	<i>m</i> -ClNB	C ₇ F ₁₄	0 ^d
14	<i>p</i> -FNB	Q	1.4		29	<i>p</i> -FNB	C ₇ F ₁₄	0 ^d
15	<i>p</i> -NO ₂ NB	2,6-Cl ₂ Q	1.0		30	NB	C ₇ F ₁₄	0 ^d

^aNB = nitrobenzene, Q = quinone, naphth Q = naphthoquinone, C₇F₁₄ = perfluoromethylcyclohexane. ^b(cm³ molecules⁻¹ s⁻¹) × 10⁹. ^c(cm³ molecules⁻¹ s⁻¹) × 10⁹. The following dipole moments (in Debye) and polarizabilities (in Å³) were used: *p*-NO₂NB, 15.5; *m*-NO₂NB, 3.8, 15.5; *n*-CF₃NB, 3.6, 18; NO₂, 0.3, 2.5. For ADO equations see Bowers.¹⁵ ^dk₁ < 10⁻¹² cm³ molecule⁻¹ s⁻¹.

this second, faster procedure. However, in all cases two to three different large B concentrations were used to check for consistency of the evaluated k₁.

The measured k_{1(exptl)} can be compared with the ADO theory¹⁵ predicted collision rate constants k_{ADO} also given in Table I. Good agreement of k₁ with k_{ADO} is observed for reactions involving A and B which are substituted nitrobenzenes or conjugated compounds like the substituted quinones and naphthoquinones. Notable is the comparison for B = *m*-dinitrobenzene and B = *p*-dinitrobenzene. Due to the presence of a dipole in the meta compound and its cancellation in the para case, ADO predicts a k_{ADO(meta)} > k_{ADO(para)}, and this trend is quantitatively followed by the experimental rate constant (see reactions 1–4, Table I). A large rate constant is observed also for the dipolar *m*-(trifluoromethyl)nitrobenzene reactions 5 and 6 in Table I.

Reactions 7–12 involving B = NO₂ and A = nitrobenzenes and quinones also proceed at (near) ADO collision efficiency. The rate constants for B = NO₂ are lower by a factor of about 2 than those for B = *p*-dinitrobenzene and most of the other B compounds with high polarizability. This is a consequence of the relatively much lower polarizability of NO₂ and the smallness of its permanent dipole moment (see Table I).

Perfluoromethylcyclohexane (C₇F₁₄) was found to have unusual behavior. This compound captures electrons most readily with a large electron capture rate constant.¹⁶ However, it is totally unreactive in many electron-transfer reactions 1 either as electron donor or electron acceptor. Typical experimental behavior for this compound is shown in Figure 5. Superficially, the intensity time dependence appears similar to that observed when there is a rapid electron-transfer equilibrium (see Figure 2A). Closer inspection shows that the distance between the two logarithmic intensity plots is increasing with time due to a slightly faster disappearance of the nitrobenzene anion. A slightly faster diffusional loss of the lighter anion (perfluoronitrobenzene) is expected. Thus the curves in Figure 5 are more consistent with no reactive coupling between A⁻ and B rather than a fast equilibrium 1. A definite proof that there is no electron transfer 1 in most reactions involving the perfluoro compound was obtained by examining the intensities in runs involving this compound and many other compounds with known electron affinities. The time dependence of the intensities was like those in Figure 5. On varying the concentrations of A and B, the quotient Q₁ was found to remain constant as would be the case if equilibrium 1 was present;

$$Q_1 = \frac{[B^-][A]}{[A^-][B]}$$

however, the ΔG°₁ values evaluated with the Q₁ led to a different position of the perfluoro compound in the EA scale (Figure 1) for every different partner used. This means that equilibrium was

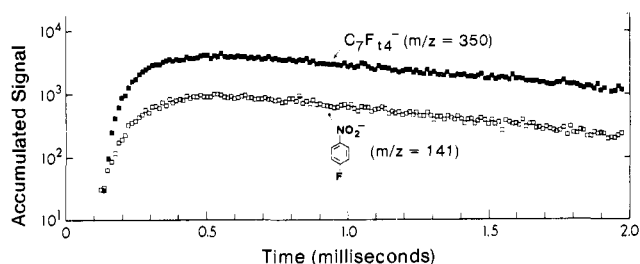


Figure 5. Intensities observed with perfluoromethylcyclohexane, C₇F₁₄ (5.9 mtorr), and *p*-fluoronitrobenzene (5.4 mtorr) in 4 torr of CH₄, 150 °C. Superficially, the intensities of the two anions appear equidistant and one might have assumed that ions are in rapid equilibrium 1, as in Figure 2, part a. However, behavior in the present system corresponds to total lack of electron transfer (eq 1).

not present in any of these cases and that the ions A⁻ and B⁻ formed by electron capture did not react at all via (1). Since electron capture by A is proportional to the concentration [A], the expression for Q₁ holds also in the complete absence of reactive equilibrium.

The C₇F₁₄⁻ did transfer electrons to some compounds B with high electron affinity (see eq 19–22, Table I). With the highest EA(2,6-Cl₂Q) = 48 kcal/mol, the electron transfer is near collision efficiency, while for the other B the efficiency of the transfer progressively decreases with decreasing EA(B), falling to near zero for B = *m*-CF₃NB with EA = 31 kcal/mol. This indicates that EA(C₇F₁₄) is smaller than EA(*m*-dinitrobenzene) = 36 kcal/mol.

In summary, the properties of C₇F₁₄ are these. It captures free near thermal electrons very readily, but it does not accept electrons from A⁻ even when the electron affinity of A is much lower than that of C₇F₁₄. C₇F₁₄⁻ transfers electrons to compounds B whose EA is higher than that of C₇F₁₄ but does so with low collision efficiency. The collision efficiency increases as EA(B) increases. This special behavior is probably associated with a large geometry change between C₇F₁₄ and the lowest energy C₇F₁₄⁻. The temperature dependence of electron transfer reactions 1 involving C₇F₁₄ and other perfluoro compounds (perfluorocyclohexane, SF₆)^{17,18} was investigated in a separate study.¹⁹ The observed magnitude and temperature dependence of the rate constants k₁ involving SF₆ could be related¹⁹ to theoretically predicted^{18b} geometry changes between SF₆ and SF₆⁻. The geometry changes for the other perfluoro compounds are not available; however, it is very likely that the kinetic model used¹⁹ for SF₆ applies also to these cases.

(17) Several investigators have reported¹⁸ on the lack of reactivity of SF₆⁻.

(18) (a) Streit, G. E. *J. Chem. Phys.* **1982**, *77*, 826. Fehsenfeld, F. C. *Ibid* **1971**, *54*, 438. Drzica, P. S.; Brauman, J. I. *J. Am. Chem. Soc.* **1982**, *104*, 13. (b) Hay, P. J. *J. Chem. Phys.* **1982**, *76*, 502.

(19) Grimsrud, E. P.; Chowdhury, S.; Kebarle, P. *J. Chem. Phys.*, in press.

(15) Su, T.; Bowers, M. T. *Int. J. Mass Spectrom. Ion Phys.* **1975**, *17*, 211.

(16) Christophorou, L. G. *Adv. Electron. Electron Phys.* **1978**, *46*, 55.

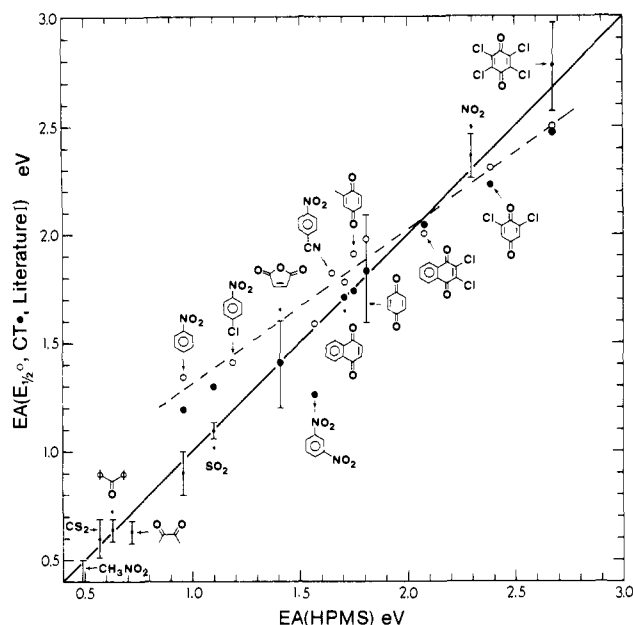
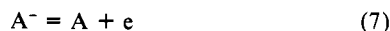


Figure 6. Comparison of electron affinities from the present work with electron affinities from other methods. Data points with error bars correspond to EA determinations in the gas phase: \circ , EA from polarographic reduction half-wave potentials $E_{1/2}$; \bullet , EA from charge-transfer spectra CT in solution. The solid line corresponds to the slope of unity, i.e., complete agreement with present data. The dashed line is the approximate observed slope for solution $E_{1/2}$ and CT data. This slope is less than unity and probably reflects decreasing solvation of anions A^- with increasing EA(A).

Compounds with low electron affinity like azulene EA = 17.3 kcal/mol (see Figure 1) have thermal electron detachment²⁰ rates (eq 7) which become appreciably faster than the diffusional loss



to the wall ν_{d,A^-} at temperatures above 200 °C. For this reason equilibria involving azulene were measured at 150 °C and those involving compounds of lower electron affinity were measured at 80 °C (see Figure 1).

Electron loss due to (7) can be a serious source of error in rate constant k_1 determinations involving A^- of compounds A with low EA, at temperatures above those where k_7 is of the same order of magnitude or larger than reaction 1 removing A^- .

(b) Electron Affinities. The electron affinities resulting from the equilibria 1 measurements are shown in Figure 1. More than half of the equilibria reported in our earlier work¹³ were redetermined. In general there was very good agreement, which resulted in only minor changes in the positions of compounds appearing in both scales. The present work provides data for 17 new compounds and extends the electron affinity scale upwards by 20 kcal/mol. The present scale is anchored to EA(SO₂) = 25.4 kcal/mol (1.1 eV) which is the electron photodetachment value due to Hall.²¹ There are four other determinations for SO₂ by different physical measurements²²⁻²⁵ which are within 0.1 eV of the above result. SO₂ lies close to the middle of the present scale, and this is another advantage in using this compound as external standard.

A comparison between the present EA's and literature data is given in Table II and Figure 6. First we consider comparisons with physical measurements of EA in the gas phase.^{4,26-28} There

is good agreement, i.e., within 0.05 eV, between the present EA values and the literature data. Thus, four literature determinations involving benzophenone,⁴ benzoquinone,²⁶ NO₂,²⁷ and chloranil (tetrachlorobenzoquinone)²⁸ show such agreement. Furthermore, the electron affinities of these compounds are evenly spread over the complete range of the present determinations (see Figure 1 and Table II). Of special interest is the agreement observed for NO₂ with the laser photodetachment value of Lineberger.²⁷ In our previous work¹³ conditions were not obtained where the NO₂⁻ to reference ion ratio in reaction 1 became constant with time. It was thought that this was due to a much too slow establishment of equilibrium 1. However, more careful examination of reaction systems involving NO₂⁻ in the present work showed that the electron-transfer equilibrium is reasonably fast, see preceding section, but that side reactions removing NO₂⁻, i.e., formation of adducts NO₂⁻B and reactions of NO₂⁻ with B were interfering.²⁹ By more careful choice of the concentration conditions, and the use of higher temperature (215 °C), good equilibria 1 involving NO₂⁻ were obtained. The resulting ΔG°_1 , see Figure 1, were used to evaluate ΔH°_1 by estimating ΔS°_1 by considering the change of multiplicity. Since NO₂ = B is a doublet and NO₂⁻ is a singlet, while A⁻ is a doublet and A a singlet, $\Delta S^\circ_1 = R \ln(1/4)$ and this leads to the $T\Delta S^\circ_1$ change shown in Figure 1, used to obtain the corresponding ΔH°_1 . No ΔS°_1 corrections were made for any of the other compounds since there are no changes of multiplicity in these cases.

A comparison of the present results with electron affinities derived from polarographic half-wave potentials ($E_{1/2}$) and charge-transfer-complex spectroscopic measurements (E_{CT}) measured in solution is also given by the data in Table II and Figure 6. These solution-derived electron affinities are from Chen and Wentworth,³⁰ who, following Briegleb,² Peover,³¹ and Bateley and Lyons,⁵ obtained the data by adjusting the constant $C_{1/2}$ and C_{CT} in eq 8 and 9 so as to obtain a best fit with available gas-phase

$$-E_{1/2} = EA - \Delta G^\circ_s - \text{constant} = EA - C_{1/2} \quad (8)$$

$$E_{CT} = I_p - EA + \Delta G^\circ_s + C = I_p - EA + C_{CT} \quad (9)$$

$$\Delta G^\circ_s = \Delta G^\circ_s(A^-) - \Delta G^\circ_s(A) \quad (10)$$

electron affinities. Examining the resulting EA in Figure 6, one finds fair agreement with the present results. The solution-derived EA's are generally somewhat higher for compounds with low EA and lower for compounds with high EA which leads to a slope which is less than unity. The solution EA depends on the assumption that the solvation difference ΔG°_s given by (10), where $\Delta G^\circ_s(X)$ is the solvation free energy of species X, is constant for all compounds. Since the solvation of A⁻ is more exothermic than that of A, ΔG°_s is negative. Higher electron affinity for the compounds present in Figure 6 is largely achieved through more extensive conjugation and increased number of electron-withdrawing substituents. Both factors disperse the negative charge in A⁻ over a large number of atoms. It is well-known that such charge delocalization leads to a decrease of the solvation exothermicity of A⁻. Since the solvation energy of the ion is dominant over that of the neutral, this should lead to an increase of ΔG°_s with increasing EA (i.e., decrease in the absolute value ($|\Delta G^\circ_s|$)). This increase is not taken into account in the one constant parameter in eq 8 and 9 and it is probably this neglect of the changing solvation that leads to the less than unit slope observed

(26) Cooper, C. D.; Naff, W. T.; Compton, R. N. *J. Chem. Phys.* **1975**, *63*, 2752. Compton, R. N.; Reinhardt, P. W.; Cooper, C. D. *Ibid.* **1974**, *60*, 2953.

(27) Herbst, E.; Patterson, T. A.; Lineberger, W. C. *J. Chem. Phys.* **1974**, *61*, 1300.

(28) Cooper, C. D.; Frey, W. F.; Compton, R. N. *J. Chem. Phys.* **1978**, *69*, 2367.

(29) The adducts of NO₂⁻ and the reactions of NO₂⁻ with 2,6-dichlorobenzoquinone and dinitrobenzene are of mechanistic interest and will be the subject of a separate publication.

(30) Chen, E. C.; Wentworth, W. E. *J. Phys. Chem.* **1975**, *63*, 3183. Becker, R. S.; Chen, E. *J. Chem. Phys.* **1966**, *45*, 2403.

(31) Peover, M. E. *J. Chem. Soc.* **1962**, 2540.

(20) Wentworth, W. E.; Chen, E.; Lovelock, J. E. *J. Phys. Chem.* **1966**, *70*, 445. Wojnarovits, L.; Foldiak, G. *J. Chromatogr.* **1981**, *206*, 511.

(21) Celotta, R. J.; Bennett, R. A.; Hall, J. L. *J. Chem. Phys.* **1974**, *60*, 1740.

(22) Hughes, B. M.; Lifshitz, C.; Tiernan, T. O. *J. Chem. Phys.* **1973**, *59*, 3182.

(23) Feldman, D. Z. *Naturforschung Teil A* **1970**, *25*, 621.

(24) Refaey, R. M. A.; Franklin, J. L. *J. Chem. Phys.* **1976**, *65*, 1994.

(25) Rothe, E. W.; Tang, S. Y.; Reck, G. R. *J. Chem. Phys.* **1971**, *62*, 3829.

Table II. Electron Affinities³⁸

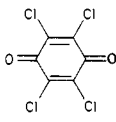
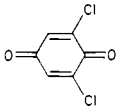
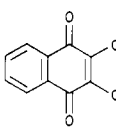
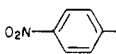
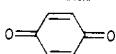
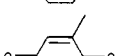
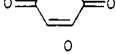
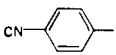
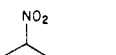
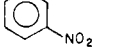
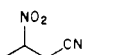
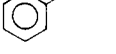
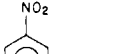
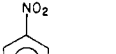
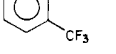
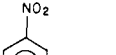
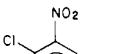

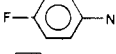
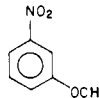
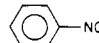
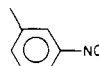
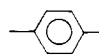
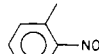
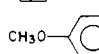
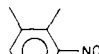
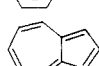
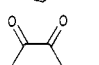
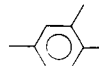
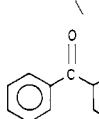
compound	EA(HPMS) ^a		EA($E_{1/2}$), ^b eV	EA(CT), ^c eV	EA(lit), eV	negative ion lifetime, ^h 10^{-6} s
	kcal	eV				
	61.9	2.68	2.48	2.44	2.76 ± 0.2^d	
	55.1	2.39	2.31	2.23	2.3^d	
NO ₂	53.3	2.31			2.36 ± 0.1^e	
	47.9	2.08	2.00	2.04		
	43.6	1.89				421
	41.7	1.81	1.98	1.83	1.89 ± 0.2^g	
	40.4	1.75	1.91	1.74		
	39.5	1.71	1.78			350
	38.0	1.65	1.82			205
	36.2	1.57	1.58	1.26		537
	35.1	1.52				209
	34.1	1.48				315
	32.4	1.41			1.39 ± 0.22^g	250
	30.9	1.34				187
	28.1	1.22				47
	27.5	1.19	1.41			14
	27.3	1.18				28
SO ₂	25.4	1.10		1.38	1.097 ± 0.036^f	2.00
	25.0	1.08				17
	24.3	1.05				10
	23.5	1.02				17

Table II (Continued)

compound	EA(HPMS) ^a		EA($E_{1/2}$), ^b eV	EA(CT), ^c eV	EA(lit), eV	negative ion lifetime, ^h 10^{-6} s
	kcal	eV				
	22.7	0.98				52
	22.1	0.97	1.34	1.19	$>0.7 \pm 0.2^j$	40
	21.4	0.93				19
	20.5	0.89				14
	20.0	0.87				13
	19.6	0.85				10
	18.7	0.81				
	17.3	0.75			0.66 ⁱ	7 ± 1.5
	16.7	0.72			0.63 ± 0.05^k	
	15.4	0.67				
	14.6	0.63			0.64 ± 0.05^k	
CS ₂	12.1	0.52			0.60 ± 0.09^k	
CH ₃ NO ₂	11.2	0.49			0.45 ± 0.09^k	

^a Present work from Figure 1. ^b EA deduced from polarographic half-wave reduction potential measurements, Chen and Wentworth.⁶
^c EA deduced from charge-transfer-complex spectra, Chen and Wentworth.⁶ ^d Cooper.²⁸ ^e Lineberger.²⁷ ^f Celotta.²¹ ^g Compton, Reinharadt, Cooper.²⁶ ^h Christophorou.²⁰ ⁱ Becker and Chen.³⁰ ^j Hughes and Lifshitz.²² ^k Chen.⁴

in Figure 6. Peover,³¹ who produced most of the half-wave potential data used in Figure 6, did the measurements in dipolar aprotic solvents like acetonitrile. The solvation of negative ions with charge dispersal in the ion is known³² to decrease least in such solvents. Solvation of negative ions in protic solvents decreases much more with charge dispersal, and had such solution data been used, a much smaller slope, i.e., a much larger deviation from unit slope in Figure 6, would have been observed.

Also given in Table II are the autodetachment lifetimes of the negative ions, after capture of near thermal electrons in the absence of third-body stabilization. The lifetimes, from experimental measurements by various authors using the time of flight mass spectrometer or electron swarm technique, were collected by Christophorou¹⁶ (Table VII, ref 16). The lifetimes increase with electron affinity, from tens of microseconds for compounds with low EA to hundreds of microseconds for high EA. Christophorou et al.¹⁶ have applied unimolecular kinetics statistical theory using essentially the RRKM³³ formalism to the special case of the "chemically activated" autodetachment process. Expressions with various levels of approximations were obtained. These predict an increase of lifetimes with increasing EA and internal degrees of freedom of A; however, the predictions are only in qualitative agreement with experiment. It is not clear whether the quantitative failure of the theory was due to the approximations used or unapplicability of the statistical theory. Christophorou et al. were handicapped by the almost complete lack of reliable experimental

data on electron affinities (see Table IX and Figure 26 in ref 16) and lack of other basic information on the properties of the anions. The present electron affinities and results from the electron-transfer kinetics can be of significant benefit. For example, the particularly simple expression 11 was obtained by Christophorou et al.¹⁶ for the (relative) lifetimes τ of substituted nitrobenzene anions, where N is the number of internal degrees of freedom in

$$\tau \propto (\text{EA})^{N-1} \quad (11)$$

the molecule. While a fair linear correlation was obtained between $(\tau)^{-(N-1)}$ and EA values (actually polarographic half-wave potentials due to lack of EA data at that time), there are some unexplained features. Thus the experimentally measured lifetimes of dinitrobenzene anions increase in the order para, meta while the electron affinities increase in the opposite order and the same is true for the corresponding cyanonitrobenzenes. Equation 11 applied to a given pair of isomers for which N is (assumed) constant predicts a higher τ for the higher EA compounds, i.e., the para isomer. This discrepancy can be resolved when one considers the situation in greater detail. As will be shown below, the greater EA of the *p*-nitro isomer is due to π electron pair withdrawal by the substituent. This decreases the negative charge near the nitro group which carries much of the excess negative charge, and a stabilization of the anion results (see structures I and II below). An equivalent stabilization is not possible in the meta isomer. However, the π electron withdrawal forms a partial double bond between the substituents and the aromatic carbons and this introduces additional hindrance for rotation around that bond. A significant reduction of the density of states of the anion

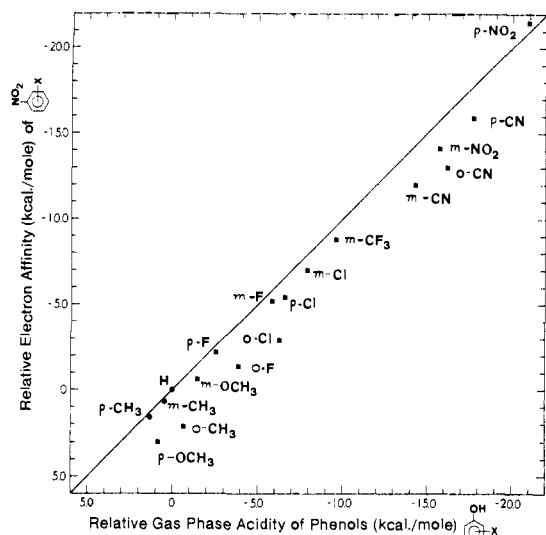


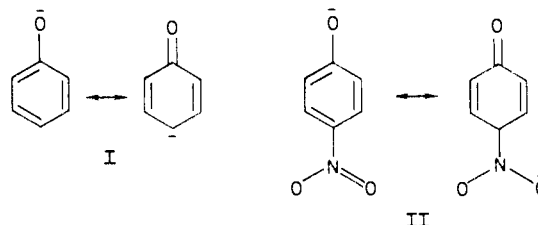
Figure 7. Comparison of relative electron affinities of substituted nitrobenzenes $X\text{-NB}$, $EA(X\text{-NB}) - EA(\text{NB})$, with relative gas-phase acidities of substituted phenols $X\text{-PhOH}$, $D(X\text{-PhP}^-\text{H}^+) - D(\text{PhO}^-\text{H}^+)$. The near unit slope demonstrates similarity of electronic effects of substituents on the nitrobenzene radical anion and the phenoxide anion. Ortho substituents are noticeably shifted further downwards than other substituents, i.e., produce a lesser stabilization of nitrobenzene anion relative to the corresponding phenoxide anion. This probably reflects decreased conjugation in nitrobenzene anions due to twisting and out of plane bending due to steric repulsion between the bulky NO_2 group and the ortho substituent.

may be expected due to loss of rotation, and this results in a decrease of the lifetime for autodetachment. This change of density of states is not taken into account by the simple expression 11.

The kinetics measurements of electron transfer reactions 1 described in the preceding section showed that perfluorocycloalkanes behave anomalously, and a suggested possible cause for this behavior was an extremely large geometry change between A and A^- . Such large changes, if true, will also have to be taken into account in the evaluation of the negative ion lifetimes of perfluorinated anions. Christophorou's lifetime evaluations of perfluorinated compounds¹⁶ did not include such considerations.

The relative electron affinities of substituted nitrobenzenes plotted vs. the relative gas-phase acidities of substituted phenols are shown in Figure 7. The electron affinities are present results from Figure 1. While phenol gas-phase acidities were first determined in this laboratory,³⁴ a more recent and complete set due to Taft et al.³⁵ is used in Figure 7. The results show not only a linear correlation but also a slope of near unity, which means that the effects of the substituents are almost identical in the two systems. Fukuda and McIver¹² were the first to use this type of plot and demonstrate the above dependence. The reader interested in a more complete discussion is referred to that work. The present figure, containing seven additional compounds including the ortho substituents, is somewhat more complete. As pointed out by McIver¹² and others,^{36,37} the extra electron in the nitrobenzene

radical anion is in a π^* -type orbital which extends over the nitro group and the aromatic ring. MO calculations and experimental spin density distributions locate ~ 0.4 electron charges on the aromatic ring and predict larger densities in positions ortho and para to the NO_2 group. This electron charge distribution is very similar to that observed for the phenoxide anions, and this similarity largely explains the correlation between the substituent effects observed in Figure 7. π electron withdrawing substituents like CN and NO_2 in ortho and para positions relative to NO_2 in the nitrobenzene anion or O^- in the phenoxides decrease the electron density in this position and are thus specially effective in stabilizing the anion.³⁷ The structures are shown below for phenoxide (I) and the *p*-nitrophenoxide (II).



The stabilizing effect of π electron withdrawing groups in the para position is larger than that for the ortho position in phenoxide ions and as the present results show, this is also true for the nitrobenzene radical anions (see *o*- and *p*-cyanonitrobenzene). Part of this effect may be due to electrostatic repulsion in the ortho ion between the two partially negatively charged groups. Additional destabilization of the ortho anion occurs due to sterically caused out of plane bending or twisting of the two hetero groups, which reduces the π conjugation with the ring. This effect has long been known and is particularly to be expected for the ortho substituted nitrobenzene radical anions³⁵ due to the large size of the nitro group. Destabilization of the nitro anion due to this steric effect occurs not only with electron withdrawing substituents but also with any other bulky substituents in the ortho position which will sterically interfere with the nitro group. Examination of Figure 7 shows that all ortho substituted compounds are relatively more shifted to the right, i.e., to larger stabilities of the *o*-phenoxy relative to the *o*-nitrobenzene anion. This follows the expected larger steric destabilization of the nitrobenzene anions relative to the phenoxides due to the larger size of the nitro group when compared to the oxy group.

Acknowledgment. This work was supported by a grant from the Canadian Natural Sciences and Engineering Research Council.

Registry No. NB, 98-95-3; NB^- , 12169-65-2; *m*- CF_3NB , 98-46-4; *m*- CF_3NB^- , 34526-71-1; *p*-FNB, 350-46-9; *p*-FNB $^-$, 34467-53-3; *p*-MeNB $^-$, 34509-96-1; *p*-ClNB $^-$, 34473-09-1; *m*- NO_2NB , 99-65-0; *m*- NO_2NB^- , 34509-56-3; *p*- NO_2NB , 100-25-4; *p*- NO_2NB^- , 34505-33-4; Q, 106-51-4; Q $^-$, 3225-29-4; 2,3- Cl_2 naphth Q, 117-80-6; 2,3- Cl_2 naphth Q $^-$, 22062-59-5; 2,6- Cl_2Q , 697-91-6; 2,6- Cl_2Q^- , 34537-54-7; C_7F_{14} , 355-02-2; C_7F_{14} , 96759-86-3; *m*-MeNB, 99-08-1; $\text{Cl}_4\text{-Q}$, 118-75-2; *m*-ClNB, 121-73-3; *o*-CNNB, 612-24-8; *p*-CNNB, 619-72-7; *m*-FNB, 402-67-5; *o*-ClNB, 88-73-3; *o*-FNB, 1493-27-2; *m*-MeONB, 555-03-3; *p*-MeONB, 100-17-4; NO_2 , 10102-44-0; azulene (radical ion 1^-), 34509-94-9.

(37) Pross, A.; Radom, L.; Taft, R. W. *J. Am. Chem. Soc.* **1980**, *102*, 818.

(38) Recent measurements of the temperature dependence of the equilibrium constants K_1 provide, via van't Hoff plots, ΔS^\ddagger_1 values. An entropy ladder was obtained which was anchored to SO_2 . The entropy change $S^\circ(\text{SO}_2^-) - S^\circ(\text{SO}_2) = 2$ eu evaluated from literature data can then be used to evaluate ΔH° values for the reaction $\text{B}^- = \text{B} + e$ and thus more accurate EA(B) than those given in Figure 1 and Table II. The substituted nitrobenzenes and quinones end up having electron affinities which are 1 to 2 kcal/mol higher than those given in Figure 1 and Table II. (Chowdhury, S.; Grimsrud, E. P.; Kebarle, P., to be published.)

(33) Robinson, P. J.; Holbrook, K. A. "Unimolecular Reactions"; Wiley-Interscience: New York, 1972.

(34) McMahon, T. B.; Kebarle, P. *J. Am. Chem. Soc.* **1977**, *99*, 2222.

(35) Fujio, M.; McIver, R. T.; Taft, R. W. *J. Am. Chem. Soc.* **1981**, *103*, 4017.

(36) Geske, D. H.; Ragle, J. L.; Bambeneck, M. A.; Balch, A. L. *J. Am. Chem. Soc.* **1964**, *86*, 987. Rieger, P. H.; Fraenkel, G. K. *J. Chem. Phys.* **1963**, *39*, 609.